Effects of Particle Concentration and Slurry Height on Gas Holdup in a Slurry Bubble Column

Shohei Sasaki, Kengo Uchida, Kosuke Hayashi and Akio Tomiyama

Graduate School of Engineering, Kobe University, 1-1 Rokkodai Nada, Kobe-shi, Hyogo 657-8501, Japan

Keywords: Slurry Bubble Column, Gas Holdup, Initial Slurry Height, Froude Number

Total gas holdups α_G in a cylindrical slurry bubble column were measured at various values of the superficial gas velocity J_G, the mean particle volumetric concentration C_S and the initial slurry height H_0 to investigate their effects on α_G. The column diameter D_H and height were 200 mm and 2000 mm, respectively. The gas, liquid and solid phases were air, water and hydrophilic silica particles of 100 μm in mean diameter, respectively. Experimental conditions were $0.025 \leq J_G \leq 0.40$ m/s, $0 \leq C_S \leq 0.50$ and $1.5 \leq H_0^* \leq 5.0$, where $H_0^* = H_0/D_H$. The conclusions obtained are as follows: (1) α_G decreases with increasing H_0 and becomes independent of H_0 for $H_0^* > 4$ at low J_G, whereas it depends on H_0 at higher J_G even for $H_0^* > 4$, (2) the increase in C_S decreases α_G up to $C_S \sim 0.40$, whereas α_G becomes independent of C_S at larger C_S, and (3) α_G in the slurry bubble column at various C_S, H_0 and J_G are well correlated in terms of the Froude number Fr_H using H_0 as a characteristic length.

Introduction

Slurry bubble column reactors have been utilized in various chemical plants for petrochemical, biochemical and metallurgical engineering applications (Degaleesan *et al.*, 2001). The total gas holdup, α_G, is one of the key parameters in designing bubble columns, and therefore, many studies on α_G have been carried out (Koide *et al.*, 1984; Khare and Joshi, 1990; Krishna *et al.*, 1997; Li and Prakash, 1997; Gandhi *et al.*, 1999; Vandu *et al.*, 2004; Mena *et al.*, 2005). These studies have confirmed that α_G depends on the superficial gas velocity, J_G, the mean particle volumetric concentration, C_S, and the initial slurry height, H_0.

It is well known that α_G decreases with increasing C_S of hydrophilic particles (Koide *et al.*, 1984; Li and Prakash, 1997; Gandhi *et al.*, 1999; Mena *et al.*, 2005; Ojima *et al.*, 2014, 2015). Since the bubble frequency in a bubble column decreases with increasing C_S, it has been speculated that the α_G reduction is due to the enhancement of bubble coalescence. In our previous studies (Ojima *et al.*, 2014, 2015), the effects of hydrophilic particles on bubble coalescence were quantitatively investigated using a two-dimensional vessel. Measurements of the time, t_C, elapsed from bubble contact to coalescence made clear that the presence of hydrophilic particles enhances bubble coalescence. The dependency of t_C on C_S was similar to that of the bubble frequency in a three-dimensional bubble column. Therefore a coalescence enhancement factor was modeled using the t_C data and implemented into a multi-fluid model. This model was validated up to $J_G = 0.034$ m/s.

In contrast to the studies on the effects of J_G and C_S, few studies have been carried out on the effects of H_0. Koide *et al.* (1984) measured α_G in a slurry bubble column at various H_0^*, where H_0^* is the ratio of H_0 to the hydraulic diameter D_H of the column. The gas holdup decreases with increasing H_0^* for $H_0^* < 7$, whereas it does not depend on H_0^* for $H_0^* \geq 7$. They proposed a gas holdup correlation for $H_0^* \geq 7$ to exclude the H_0 effect. Though several α_G correlations have been proposed for slurry bubble columns (Li and Prakash, 1997; Krishna *et al.*, 1997; Gandhi *et al.*, 1999; Vandu *et al.*, 2004), no discussion on how to account for the H_0 effect in α_G correlations has been made.

In our previous study (Sasaki *et al.*, 2016), we investigated the effects of H_0^* on α_G in air-water bubble columns of $D_H = 200$ mm for a wide range of J_G and H_0, i.e., $0.025 \leq J_G \leq 0.40$ m/s and $1.5 \leq H_0^* \leq 5.0$. The α_G data were well correlated in terms of the Froude number Fr_H defined by using H_0 as the characteristic length. The applicability of Fr_H in correlating α_G in slurry bubble columns, however, has not been examined yet.

In this study, gas holdups in a slurry bubble column were measured at various values of J_G and C_S and for $H_0^* \leq 5.0$ to investigate their effects on α_G. The applicability of Fr_H to α_G in the slurry bubble column was also examined.

1. Experimental

1.1 Experimental setup

Figure 1 shows the experimental setup. The cylindrical column was made of transparent acrylic resin for flow visualization. The column height was 2000 mm, and D_H was 200 mm.

The column was initially filled with slurry consisting

Received on November 4, 2015; accepted on May 9, 2016
DOI: 10.1252/jcej.15we280
Correspondence concerning this article should be addressed to A. Tomiyama (E-mail address: tomiyama@mech.kobe-u.ac.jp).

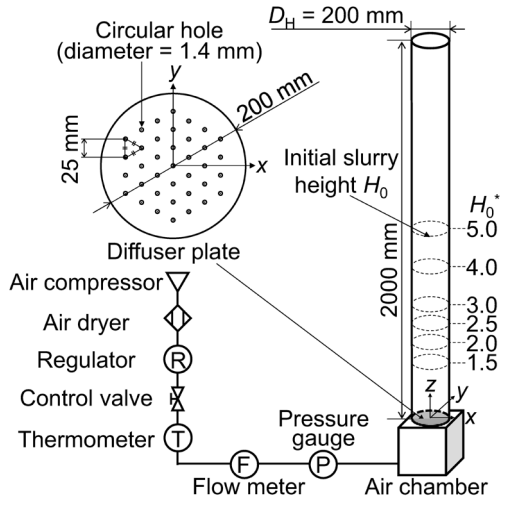

Fig. 1 Experimental setup

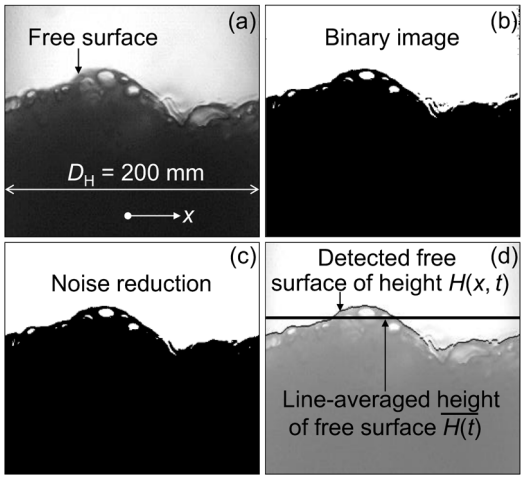

Fig. 2 Image processing for α_G measurement ($J_G = 0.050$ m/s, $H_0^* = 5.0$, $C_S = 0.20$)

of water and fine particles. Water at room temperature (19±1°C) and atmospheric pressure was used for the liquid phase. Hydrophilic spherical silica particles (CARiACT®, Q-10, Fuji Silysia Chemical Ltd.) were used for the solid phase. The mean diameter, d_P, true density, ρ_S, apparent density, ρ_P, and pore volume, θ, of the particles were 100 μm, 2250 kg/m^3, 1320 kg/m^3 and 1.3×10^{-3} m^3/kg, respectively, where the apparent density was evaluated by taking the volume-weighted average of the true density and the density of water filling its pore volume. The porosity, δ, of the particles defined by $\delta = \rho_S\theta/(1+\rho_S\theta)$ is 0.75. Since the pore of silica particles could be filled with water, the total particle volume in the slurry was defined as $V_S+\Theta$, where V_S is the total volume of the solid phase in the slurry and Θ the total volume of the pore of particles. The mean particle concentration, C_S, of the slurry was, therefore, defined by $C_S = (V_S+\Theta)/V_{SL}$, where V_{SL} ($=\pi D_H^2 H_0/4$) is the slurry volume. The C_S can also be expressed as $C_S = \theta M_S/V_{SL}\delta$, where M_S is the total mass of the solid phase. The C_S ranged from 0 to 0.50. The uncertainty in C_S at 95% confidence was 0.01.

Air supplied from the compressor (RDG-150C, Anest Iwata Corp.) flowed into the column through the air dryer (SLP-1501EB, Anest Iwata Corp.) and the air chamber. The air diffuser plate of 5 mm in thickness was placed at the bottom of the column. The hole diameter, the number of holes, the hole pitch and the ratio of the total hole area to the area of column cross-section were 1.4 mm, 37, 25 mm and 0.18%, respectively.

The gas volume flow rate was measured using the flowmeters (NVP-I, FLT-H, Nippon Flow Cell Co., Ltd.; AM-1000, full-scale accuracy ±1.5%, Tokyo Keiso Co. Ltd.). The measured flow rate was converted into the volume flow rate at the middle height of the slurry level by taking into account gas expansion due to the decrease in static pressure. The range of J_G defined at the latter location was from 0.025±0.001 to 0.40±0.01 m/s, where the uncertainties were evaluated at 95% confidence.

The physical properties of the gas and liquid phases are as follows: the liquid density was 998 kg/m^3, the gas density 1.2 kg/m^3, the liquid viscosity, μ_L, 1.0×10^{-3} Pa·s, the gas viscosity 1.8×10^{-5} Pa·s, and the surface tension 0.072 N/m. The initial slurry height, H_0, was varied from 300 to 1000 mm. The ratio, H_0*, of H_0 to D_H, therefore, ranged from 1.5 to 5.0. Since the Stokes number, St ($=\rho_P d_P^2 J_G/18\mu_L D_H$) (Ojima *et al.*, 2015), was much smaller than unity, e.g., $St = 7.3\times10^{-4}$ at $J_G = 0.20$ m/s, and bubbles strongly stirred the slurry, the particle concentration would be uniform in the column.

1.2 Measurement method

The gas holdup of the bubble column was measured by processing images of the free surface. The images were taken using a high-speed video camera (Motion Pro X-3, Integrated Device Technology Inc.) with spatial and temporal resolutions of 0.36 mm/pixel and 1/100 s, respectively. As shown in **Figure 2**, they were transformed into binary images. Then, the instantaneous slurry height, $H(x, t)$, at the horizontal position x and the time t was detected using a region growing method (Hojjatoleslami and Kittler, 1998) after noise reduction. The mean slurry height at t was calculated as

$$\overline{H(t)} = \frac{1}{D_H}\int_{-D_H/2}^{D_H/2} H(x,\ t)\mathrm{d}x \tag{1}$$

The total gas holdup was then calculated as

$$\alpha_G = \frac{1}{T}\int_{t_1}^{t_1+T} \frac{\overline{H(t)}-H_0}{\overline{H(t)}}\mathrm{d}t \tag{2}$$

where t_1 is the time, at which the recording was started, and T the sampling time. Instantaneous and time-averaged $\overline{H(t)}$ at $J_G = 0.40$ m/s in the slurry bubble column are shown in **Figure 3**. For the latter, T was varied from 0 to 30 s to examine the convergence of the time-averaged value. The instantaneous $\overline{H(t)}$ fluctuates largely, whereas the time-averaged $\overline{H(t)}$ at $T = 30$ s converges to within ±0.5% de-

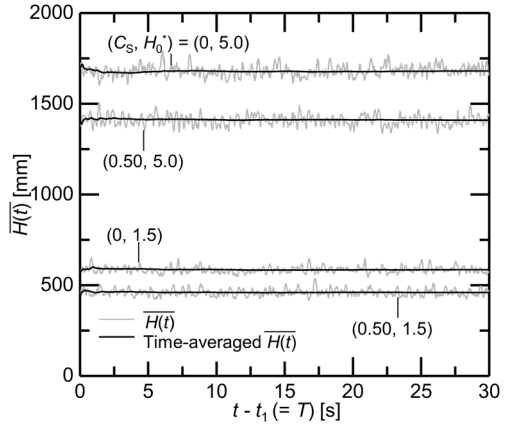

Fig. 3 Instantaneous and time-averaged $\overline{H(t)}$ at $J_G = 0.40$ m/s

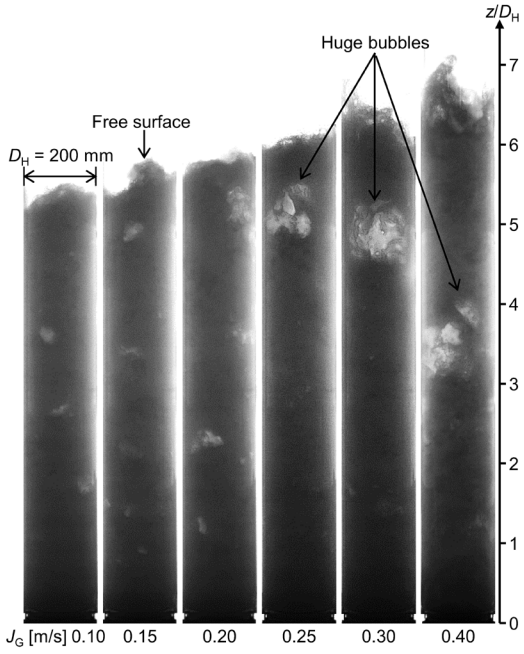

Fig. 4 Bubbly flows at $C_S = 0.20$ and $H_0^* = 5.0$

viations. In the following, α_G data evaluated using $T = 30$ s in Eq. (2) are presented. The relative standard errors in α_G were evaluated by repeating the measurement 10 times under the conditions of $C_S = 0$ and 0.50, $J_G = 0.025$ and 0.40 m/s, and $H_0^* = 1.5$ and 5.0. The errors in α_G were within $\pm 1\%$.

The flow was observed by using a high-speed video camera (Fastcam SA-X2, Photron Ltd.). Four fluorescent lights were used for back illumination. The shutter speed and the frame rate were 1/20000 and 500 fps, respectively. The sampling time was 20 s. The spatial resolution of the flow visualization was 0.49 mm/pixel.

2. Results and Discussion

2.1 Flow structure and gas holdup

Typical images of bubbles in the slurry at $H_0^* = 5.0$ and $C_S = 0.20$ are shown in **Figure 4**. Though the presence of

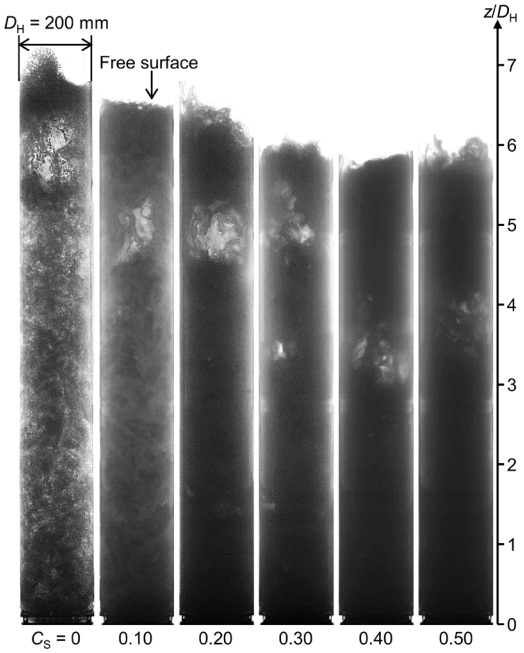

Fig. 5 Bubbly flows at $J_G = 0.30$ m/s and $H_0^* = 5.0$

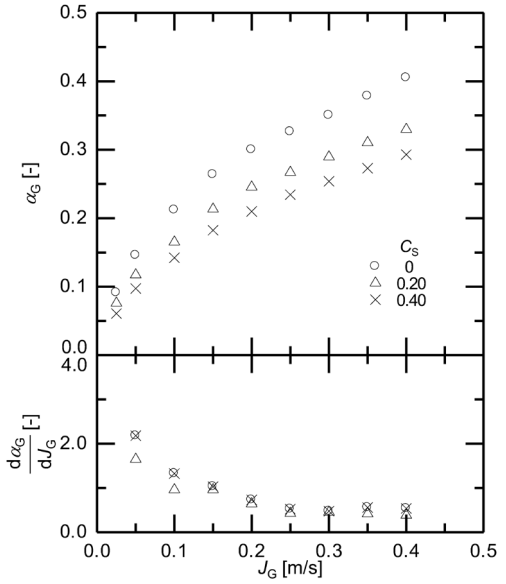

Fig. 6 Total gas holdup α_G and gradient $d\alpha_G/dJ_G$ at $H_0^* = 5.0$

particles strongly deteriorates the transparency of slurry, high-speed video images confirmed that the flows were heterogeneous. For $J_G > 0.20$ m/s, huge bubbles were formed at $z/D_H \sim 2$, where z is the vertical distance from the bottom of the column. The huge bubbles strongly agitated the flow over the whole column cross section. This trend was similar to that at $C_S = 0$ in Sasaki *et al.* (2016). The characteristics of flow structures rarely depended on C_S.

Figure 5 shows flows at $H_0^* = 5.0$ and $J_G = 0.30$ m/s. The increase in C_S decreases the height of the free surface, in other words, the total gas holdup. The heights for $C_S \geq 0.40$ are, however, almost the same.

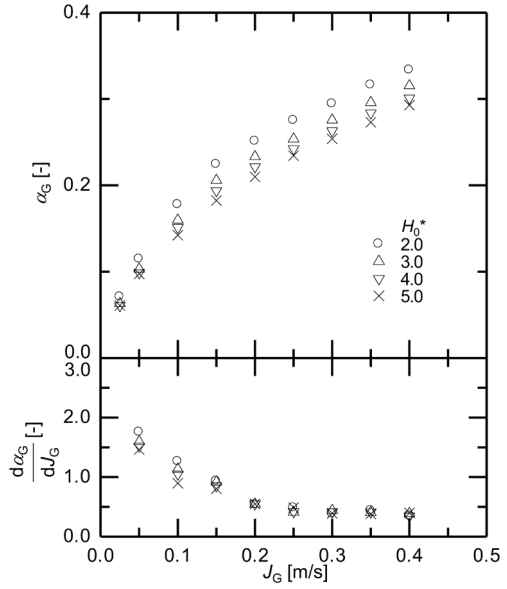

Fig. 7 α_G and $d\alpha_G/dJ_G$ at $C_S = 0.40$

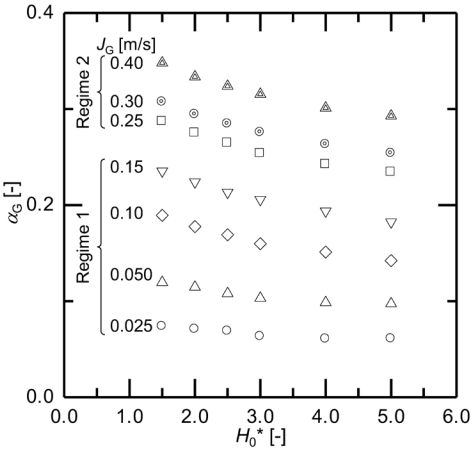

Fig. 8 Effects of H_0 on α_G at $C_S = 0.40$

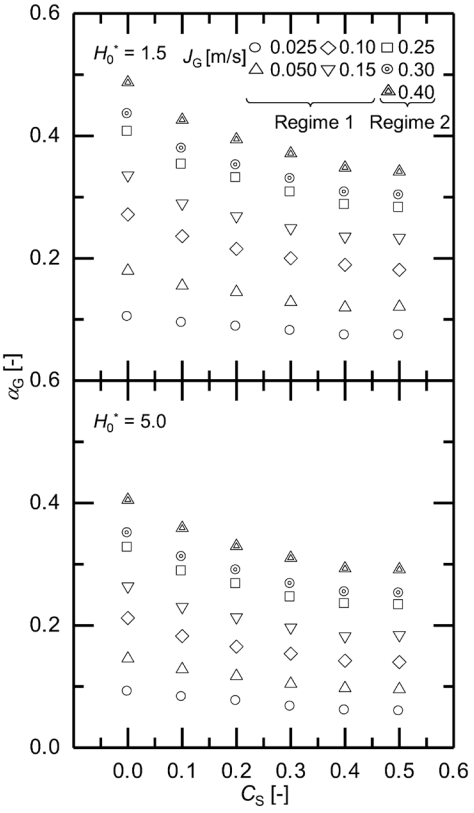

Fig. 9 Effects of C_S on α_G at $H_0^* = 1.5$ and 5.0

Gas holdups at $H_0^* = 5.0$ are shown in **Figure 6**, where the α_G data at $C_S = 0$ were quoted from Sasaki *et al.* (2016). The α_G monotonously increases as J_G increases. This trend is the same as that of the so-called pure heterogeneous flow (Ruzicka *et al.*, 2003). The increase in C_S decreases α_G. This α_G reduction is due to the bubble coalescence enhancement by hydrophilic particles (Ojima *et al.*, 2014, 2015).

Figures 6 and **7** also show $d\alpha_G/dJ_G$. The $d\alpha_G/dJ_G$ decreases with increasing J_G and depends on H_0^* for $J_G \lesssim 0.20$ m/s, whereas the dependency of $d\alpha_G/dJ_G$ on J_G and H_0^* is weak at larger J_G. The critical value of J_G corresponds to that for the formation of huge bubbles. Though all the flows in the present experiments are classified into the heterogeneous regime, the flow structure can be further divided into two regimes, i.e., flows without huge bubbles and those with huge bubbles. Hereafter, we refer to the ranges for the former and latter as Regime 1 and Regime 2, respectively (Sasaki *et al.*, 2016).

Figure 7 shows gas holdups at $C_S = 0.40$. The increase in H_0^* decreases α_G both in Regimes 1 and 2. The lower α_G at high H_0^* means that the mean bubble diameter in the column was larger compared to that at low H_0^*.

The total gas holdups are re-plotted against H_0^* in **Figure 8** to clearly show the effects of H_0 on α_G. At a constant J_G, α_G decreases with increasing H_0^*. Koide *et al.* (1984) measured α_G for $C_S \leq 0.04$. They concluded that the H_0 effect is negligible for $H_0^* > 7$. In the present data, α_G becomes independent of H_0 for $H_0^* > 4$ at low J_G, i.e. $J_G = 0.025$ and 0.050 m/s. The effect, however, appears at higher J_G even for $H_0^* > 4$.

The C_S effect on α_G at $H_0^* = 1.5$ and 5.0 is shown in **Figure 9**. Due to the particle-induced enhancement of bubble coalescence, α_G decreases with increasing C_S. At $H_0^* = 5.0$, α_G for $C_S \gtrsim 0.40$ are independent of C_S. On the other hand, α_G slightly decrease with increasing C_S even for $C_S \gtrsim 0.40$ when $H_0^* = 1.5$, especially at high J_G. The reason for this difference can be understood as follows: since huge bubbles were formed at $z/D_H \sim 2$, bubble coalescence was dominant for $z/D_H \lesssim 2$. On the other hand, the bubble coalescence rate was smaller for $z/D_H \gtrsim 2$ compared to the former region. The particle effect on bubble coalescence enhancement might, therefore, be of importance in the former. The ratio of the former region to the whole flow region decreases as H_0^* increases. Hence, the increase in C_S reduces α_G even at the high C_S when $H_0^* = 1.5$.

Ojima *et al.* (2014, 2015) measured the film drainage time, t_C, i.e., the time elapsed from bubble contact to coales-

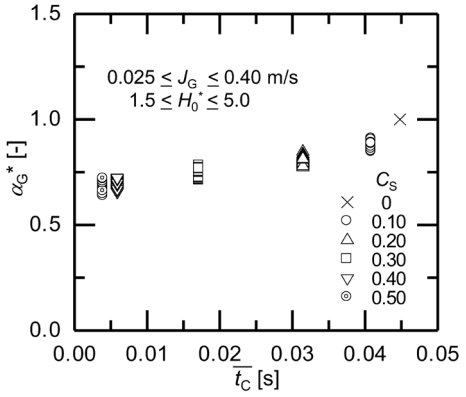

Fig. 10 Normalized gas holdup vs. film drainage time

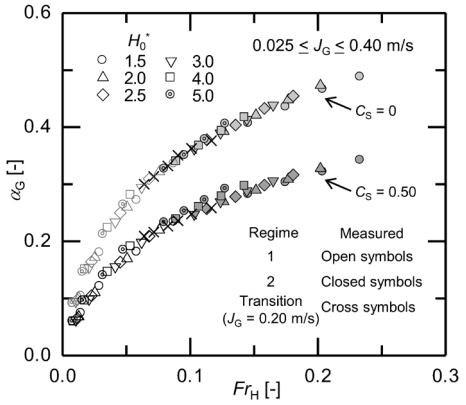

Fig. 11 α_G plotted against Fr_H

cence, to investigate the effects of hydrophilic silica particles on bubble coalescence in a quasi two-dimensional vessel. The t_C decreased with increasing C_S for $C_S < 0.45$. Hence, bubble coalescence is enhanced with increasing C_S. For $C_S \geq 0.45$, further bubble-coalescence enhancement was not observed even with increasing C_S. **Figure 10** shows a comparison between $\overline{t_C}$ in the 2D vessel and the following normalized gas holdup, α_G^*, in the cylindrical bubble column:

$$\alpha_G^* = \frac{\alpha_G(H_0^*, J_G, C_S)}{\alpha_G(H_0^*, J_G, 0)} \tag{3}$$

The strong correlation between α_G^* and $\overline{t_C}$ implies that the α_G reduction with increasing C_S in the bubble column is caused by the bubble coalescence enhancement due to the presence of particles.

2.2 Applicability of Froude Number to α_G correlation

In our previous study (Sasaki *et al.*, 2016), we confirmed that the gas holdups in air-water bubble columns for $1.5 \leq H_0^* \leq 5.0$ is well correlated in terms of the following Froude number:

$$Fr_H = \frac{J_G}{\sqrt{gH_0}} \tag{4}$$

where g is the acceleration of gravity. **Figure 11** shows α_G plotted against Fr_H. The α_G increases with increasing Fr_H.

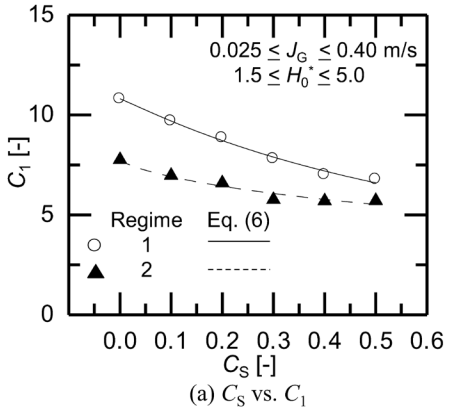

(a) C_S vs. C_1

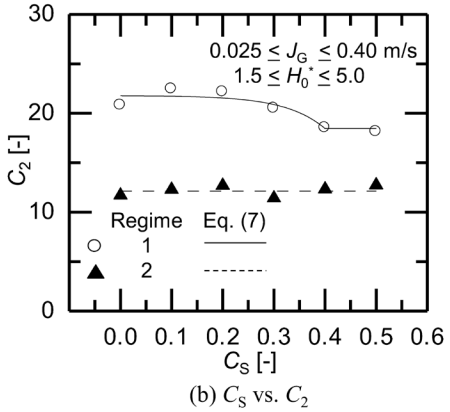

(b) C_S vs. C_2

Fig. 12 Interpolation functions of C_1 and C_2 in Eq. (5)

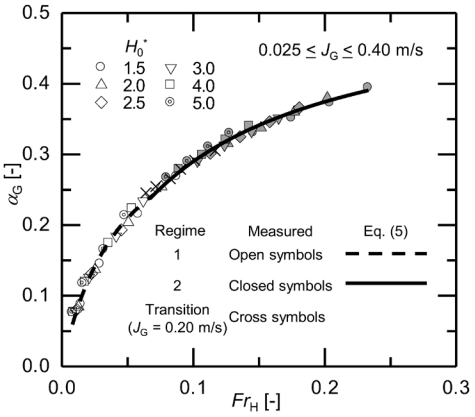

Fig. 13 α_G in the slurry bubble column correlated in terms of Fr_H at $C_S = 0.20$ (C_1 and C_2 are calculated using Eqs. (6) and (7))

The Froude number well correlates not only α_G in the air-water bubble column but also those in the slurry bubble column.

The following functional form was also used to express the α_G data in Sasaki *et al.* (2016):

$$\alpha_G^R = \frac{C_1^R Fr_H}{1 + C_2^R Fr_H} \quad (R = R_1 \text{ or } R_2) \tag{5}$$

where C_1 and C_2 are regime-dependent coefficients and the superscripts, R_1 and R_2, denote Regimes 1 and 2, respectively. Values of C_1 and C_2 determined by fitting Eq. (5) to

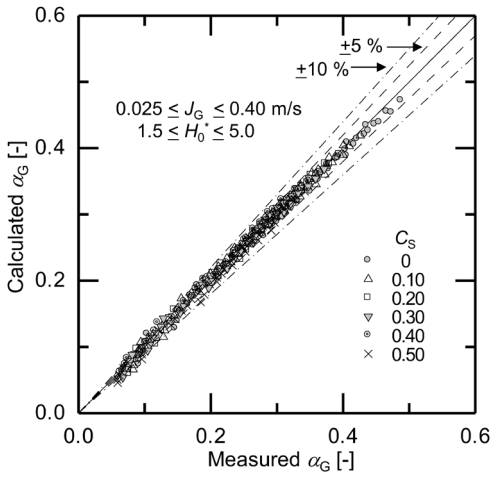

Fig. 14 Comparison between Eq. (5) and α_G data

the data are shown in **Figure 12**. In both regimes, C_1 decreases with increasing C_S, whereas it becomes constant for $C_S \geq 0.40$. This reflects the fact that the dependency of α_G on C_S is very weak for this C_S range. The C_2 in Regime 1 also decreases as C_S increases. On the other hand, C_2 in Regime 2 is constant. Interpolation functions of C_1 and C_2 in terms of C_S were obtained as

$$C_1 = \begin{cases} \dfrac{8.12}{0.75 + C_S^{1.07}} & \text{in Regime 1} \\ \dfrac{11.4}{1.47 + C_S^{0.73}} & \text{in Regime 2} \end{cases} \quad (6)$$

$$C_2 = \begin{cases} \max[21.8 - 0.018e^{13C_S}, 18.5] & \text{in Regime 1} \\ 12.2 & \text{in Regime 2} \end{cases} \quad (7)$$

Figures 13 and 14 show comparisons of the α_G data at $C_S = 0.20$ with Eq. (5) and those of all the data with Eq. (5), respectively. Equation (5), which includes only two fitting parameters C_1 and C_2, can well correlate all the data.

Conclusion

Total gas holdups, α_G, in a cylindrical slurry bubble column were measured by using a high-speed video camera and an image processing method to investigate the effects of the initial slurry height, H_0, the superficial gas velocity, J_G, and the mean particle volumetric concentration, C_S, on α_G. The column diameter, D_H, was 200 mm. Air, water and hydrophilic spherical silica particles were used for the gas, liquid and solid phases, respectively. The mean particle diameter was 100 μm. The C_S varied from 0 to 0.50. The J_G ranged from 0.025 to 0.40 m/s. The ratio, $H_0^* = H_0/D_H$, of initial slurry height to diameter was from 1.5 to 5.0. The conclusions obtained under the present experimental conditions are as follows.

1. The gas holdup decreases with increasing H_0 and becomes independent of H_0 for $H_0^* > 4$ at low J_G. The height effect, however, appears at higher J_G even for $H_0^* > 4$.
2. The gas holdup decreases with increasing C_S up to $C_S \sim 0.40$, whereas it becomes independent of C_S at larger C_S.
3. The gas holdups at various initial slurry heights are well correlated in terms of the Froude number defined by using the superficial gas velocity and the initial slurry height as the characteristic velocity and length, respectively.

Acknowledgement

This work has been supported by the Japan Society for the Promotion of Science (JSPS) (Grants-in-Aid for Scientific Research (B), No. 15H03920).

Nomenclature

C_S	=	particle volumetric concentration	[—]
C_1, C_2	=	coefficients in Eq. (5)	[—]
D_H	=	hydraulic diameter	[m]
d_P	=	mean particle diameter	[m]
Fr_H	=	Froude number ($Fr_H = J_G/\sqrt{gH_0}$)	[—]
g	=	acceleration of gravity	[m/s^2]
H_0	=	initial slurry (or liquid) height	[m]
H_0^*	=	dimensionless slurry height ($H_0^* = H_0/D_H$)	[—]
H	=	instantaneous slurry height	[m]
J_G	=	superficial gas velocity	[m/s]
M_S	=	total mass of solid phase	[kg]
St	=	Stokes number ($St = \rho_P d_P^2 J_G/18\mu_L D_H$)	[—]
t_C	=	film drainage time	[s]
t	=	time	[s]
t_1	=	time, at which video recording is started	[s]
T	=	sampling time	[s]
V_S	=	total volume of solid phase in slurry	[m^3]
V_{SL}	=	slurry volume ($V_{SL} = \pi D_H^2 H_0/4$)	[m^3]
x	=	horizontal coordinate	[m]
z	=	vertical coordinate	[m]
α_G	=	total gas holdup	[—]
α_G^*	=	normalized gas holdup	[—]
δ	=	porosity of particles ($\delta = \rho_S\theta/(1+\rho_S\theta)$)	[—]
θ	=	pore volume of particles	[m^3/kg]
Θ	=	total volume of pore of particles	[m^3]
μ_L	=	liquid viscosity	[Pa·s]
ρ_S	=	true particle density	[kg/m^3]
ρ_P	=	apparent particle density	[kg/m^3]

Literature Cited

Degaleesan, S., M. Dudukovic and Y. Pan; "Experimental Study of Gas-Induced Liquid-Flow Structures in Bubble Columns," *AIChE J.*, **47**, 1913–1931 (2001)

Gandhi, B., A. Prakash and M. A. Bergougnou; "Hydrodynamic Behavior of Slurry Bubble Column at High Solids Concentrations," *Powder Technol.*, **103**, 80–94 (1999)

Hojjatoleslami, S. A. and J. Kittler; "Region Growing: A New Approach," *IEEE Trans. Image Process.*, **7**, 1079–1084 (1998)

Khare, A. S. and J. B. Joshi; "Effect of Fine Particles on Gas Hold-Up in Three-Phase Sparged Reactors," *Chem. Eng. J.*, **44**, 11–25 (1990)

Koide, K., A. Takazawa, M. Komura and H. Matsunaga; "Gas Holdup and Volumetric Liquid-Phase Mass Transfer Coefficient in Solid-

Suspended Bubble Columns," *J. Chem. Eng. Japan*, **17**, 459–466 (1984)

Krishna, R., J. W. A. de Swart, J. Ellenberger, G. B. Martina and C. Maretto; "Gas Holdup in Slurry Bubble Columns: Effect of Column Diameter and Slurry Concentrations," *AIChE J.*, **43**, 311–316 (1997)

Li, H. and A. Prakash; "Heat Transfer and Hydrodynamics in a Three-Phase Slurry Bubble Column," *Ind. Eng. Chem. Res.*, **36**, 4688–4694 (1997)

Mena, P. C., M. C. Ruzicka, F. A. Rocha, J. A. Teixeira and J. Drahoš; "Effect of Solids on Homogeneous–Heterogeneous Flow Regime Transition in Bubble Columns," *Chem. Eng. Sci.*, **60**, 6013–6026 (2005)

Ojima, S., K. Hayashi and A. Tomiyama; "Effects of Hydrophilic Particles on Bubbly Flow in Slurry Bubble Column," *Int. J. Multiph. Flow*, **58**, 154–167 (2014)

Ojima, S., S. Sasaki, K. Hayashi and A. Tomiyama; "Effects of Particle Diameter on Bubble Coalescence in a Slurry Bubble Column," *J. Chem. Eng. Japan*, **48**, 181–189 (2015)

Ruzicka, M. C., J. Drahoš, P. C. Mena and J. A. Teixeira; "Effect of viscosity on homogeneous-heterogeneous flow regime transition in bubble columns," *Chem. Eng. J.*, **96**, 15–22 (2003)

Sasaki, S., K. Hayashi and A. Tomiyama; "Effects of Liquid Height on Gas Holdup in Air-Water Bubble Column," *Exp. Therm. Fluid Sci.*, **72**, 67–74 (2016)

Vandu, C. O., K. Koop and R. Krishna; "Volumetric Mass Transfer Coefficient in a Slurry Bubble Column Operating in the Heterogeneous Flow Regime," *Chem. Eng. Sci.*, **59**, 5417–5423 (2004)